ACS APPLIED MATERIALS & INTERFACES

Research Article

www.acsami.org

Stacked Quantum Dot Embedded Silica Film on a Phosphor Plate for Superior Performance of White Light-Emitting Diodes

In Seong Sohn,[§] Sanjith Unithrattil,[§] and Won Bin Im*

School of Materials Science and Engineering, Chonnam National University, 300 Yongbong-dong, Buk-gu, Gwangju 500-757, Republic of Korea

ABSTRACT: Application of quantum dots as a color converter in white light-emitting diodes (WLEDs) has been highly restrained because of its lower stability under the operating conditions of LEDs. The feasibility of using quantum dots in WLEDs has been studied and demonstrated by developing a non-conventional packing technique. Multiple core shell $CuInS_2$/ZnS quantum dots were coated by silica, and the silica-coated quantum dots were dispersed in ethoxylated trimethylolpropane triacrylate to form a color conversion film. This along with phosphor in a glass plate made of $Y_3Al_5O_{12}:Ce^{3+}$ phosphor was stacked in different configurations, and its effect on color rendering of WLEDs was studied. In addition, the configuration developed here protects the color converter from thermal strain and moisture.

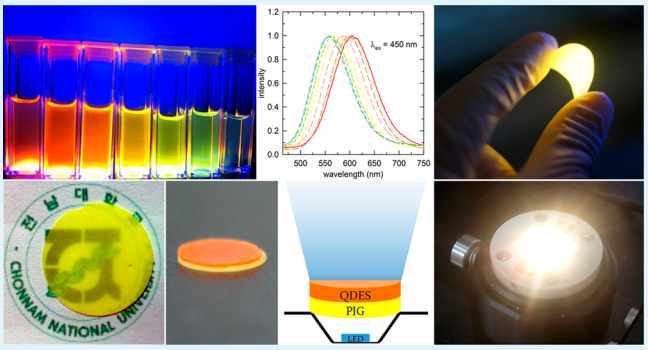

KEYWORDS: *white LEDs, packaging, quantum dots, solid-state lighting*

INTRODUCTION

White light-emitting diode (WLED) technology, after its discovery, has been riding on the $Y_3Al_5O_{12}:Ce^{3+}$ (YAG:Ce^{3+}) phosphor mainly because of its unparalleled efficacy. Because of weak red emission of YAG:Ce^{3+}, the color rendering index of the combination is far less than what is needed for a general lighting purpose. This has primarily restrained the system from widespread use, as it had envisaged a decade back. The lack of appropriate red-emitting phosphor together with inherent problems, such as reabsorption, has made the task difficult.[1−3]

Over the past several years, many red-emitting phosphors, including quantum dots (QDs) and quantum wires, have been proposed. These red-emitting phosphors, such as $CaAlSiN_3:Eu^{2+}$, $Y_2O_2S:Eu^{3+}$, etc., were seen as a good bet.[4,5] The proposed phosphors have improved the color rendering index (CRI) of the combination but at the expense of the efficacy, while QDs could not be employed because of its low stability. To overcome this, QDs have been successfully embedded in a polymer encapsulant,[6−8] silica, and glass matrix.[9−12] A few of these encapsulation techniques were employed in WLED packaging, and comparative studies have been carried out.[13−15] The mixtures of YAG:Ce^{3+} phosphor along with red components have consistently proven to yield lower efficiency, despite providing desired CRI as a result of reabsorption.[16]

In this study, we have successfully developed a new packaging technique by employing phosphor in glass (PiG) along with QDs embedded in silica and polymers. $CuInS_2$/ZnS QDs were synthesized through the heating method, and the shell formation was accompanied by timely injection of ZnS shell stock solution and subsequent stirring. After the completion of shell formation, to disperse QDs in the ethanol, ligand exchange was performed. Quantum dot embedded silica (QDES) particles were synthesized through modified sol−gel chemistry by the Stöber−Fink−Bohn method and seeded growth.[17]

EXPERIMENTAL SECTION

Luminescent polymer films were prepared by dispersing QDES in ethoxylated trimethylolpropane triacrylate (ETPTA). ETPTA was chosen to disperse the QDES because the refractive index of the polymer matches exactly with that of silica in colloidal form and, thereby, eliminates refractive dispersion of light within the system. In addition, the viscoelastic properties of the polymer ensure the least coalescence among QDES and, thereby, uniform dispersion in the polymer. QDES dispersed in ethanol was centrifuged and dried at 60 °C for about 6 h. Dried QDES was then mixed with ETPTA and photoinitiator 2-hydroxy-2-methyl-1-phenyl-2-propanone at a ratio of 1:10. The mixture was then applied on a glass slide lined with scotch tape and compressed with another glass slide of the same dimension. This arrangement was kept under ultraviolet (UV) light for 10 min, and the hardened QDES-dispersed ETPTA film (Q-ETPTA) was sliced into a thin circular disc of appropriate dimension.

Synthesis of QDs starts by loading 0.5 mmol (0.095 g) of CuI, 0.5 mmol (0.146 g) of $In(Ac)_3$, and 5 mL of 1-dodecanethiol (DDT) in 50 mL of a three-neck flask. The reaction mixture was degassed during heating to 100 °C, backfilled with Ar, and subsequently, further heated to 230 °C within 10 min. The growth of $CuInS_2$ core QDs was allowed for 5 min at that temperature. For the ZnS shell overcoating, a ZnS

Received: January 20, 2014
Accepted: March 25, 2014
Published: March 25, 2014

   dx.doi.org/10.1021/am500429c | *ACS Appl. Mater. Interfaces* 2014, 6, 5744−5748

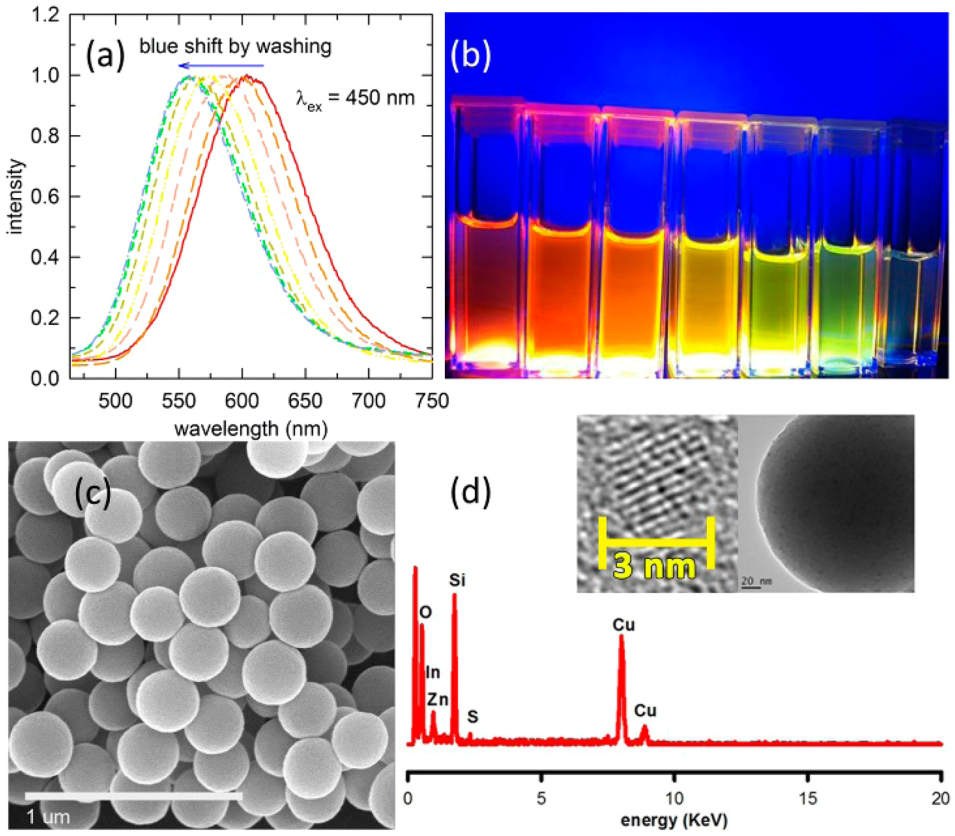

Figure 1. (a) PL emission spectra of synthesized QDs. (b) QDs under UV excitation. (c) Scanning electron microscopy (SEM) image of QDES. (d) EDS spectra of QDES. The inset of panel d shows the lattice fringes obtained from TEM.

shell stock solution, zinc undecylenate (0.3 mmol), dissolved in 1.5 mL of 1-aminodecane was injected every 30 min and stirred for 4 h to complete ZnS shell formation on the surface of $CuInS_2$ QDs.[18] Ligand-exchanged QDs dispersed in ethanol were injected into the system, 30 min after initiating the process during the initial stage of seed growth. A total of 5 mL of 3-aminopropyltrimethoxysilane was added to the system at a temperature of 140 °C, and the temperature was maintained for 10 min. The QDES matrix formed by self-silanization was then precipitated, and the particles were filtered from the solution and allowed to dry for 30 min at 65 °C. $CuInS_2$/ZnS QDs were then treated with 2 mL of MUD reaction solution and stirred for 15 min. The stirred solution was then transferred to ethanol medium, and ligand-exchanged $CuInS_2$/ZnS QDs were precipitated out by adding hexane to it. The final solution was purified using centrifugation and stored in ethanol.[19]

QDES particles were synthesized through a modified sol–gel chemistry by the Stöber–Fink–Bohn method and seeded growth.[17] Ligand-exchanged QDs dispersed in ethanol were injected into the system, 30 min after initiating the process during the initial stage of seed growth. A total of 5 mL of 3-aminopropyltrimethoxysilane was added to the system at a temperature of 140 °C, and the temperature was maintained for 10 min. QDES matrix formed by self-silanization was then precipitated, and the particles were filtered from the solution and allowed to dry for 30 min at 65 °C.

PiGs were prepared from YAG:Ce^{3+}, and glass frit was prepared from the constituents B_2O_3, Al_2O_3, SiO_2, K_2O, and ZnO in an appropriate proportion to form the $(SiO_2–ZnO–B_2O_3)–Al_2O_3–K_2O$ system, where $SiO_2–ZnO–B_2O_3$ constitutes 80 wt %, while Al_2O_3 and K_2O constitute 5 and 15 wt %, respectively. $SiO_2–ZnO–B_2O_3$ is composed of 25, 35, and 25 wt % of SiO_2, ZnO, and B_2O_3, respectively. The constituents are then mixed and homogenized to form a proper glass frit. A detailed procedure of the preparation of PiG is described elsewhere.[20,21] In brief, the glass frits were mixed with YAG:Ce^{3+} phosphor at a ratio of 3:97 by weight and then compressed into a circular disk. These were then fired at 600 °C for 30 min and naturally cooled to room temperature, and the obtained discs (Figure 3a) were polished and used for further studies.

Morphologies of the synthesized QDs and QDESs were characterized using a Hitachi S-4700 field emission scanning electron microscope. The photoluminescence (PL) measurements were carried out on a Hitachi F-4500 spectrophotometer equipped with a 150 W xenon lamp as the excitation source. Thermal quenching studies were carried out on custom-made equipment consisting of a heater, sensor, and fluorescence spectrometer. The electroluminescence (EL) spectrum of the glass plate was measured using a Dasara Pro-5200 EL spectrometer.

RESULTS AND DISCUSSION

Figure 1a shows the PL spectra of $CuInS_2$/ZnS QDs. About 3 nm sized QDs were synthesized through the heating method. The as-synthesized QDs verifying the typical color variation with size and spherical shape were obtained with monodispersity, as confirmed from the transmission electron microscopy (TEM) image shown in Figure 1d. The emission spectra consist of a broadband with peaks positioned from 550 to 600 nm, under 450 nm excitation. The measured quantum yield of synthesized QDs in solution was about 60%, with a full width at half maximum (fwhm) of 102 nm. The ligands were exchanged to hydroxyl-functionalized ligands to make QDs disperse in polar solvents. QDs collected by precipitating out show red emission because of their enlarged size, as compared to the as-prepared QDs. By embedding QDs in silica, we successfully achieved QDES through a Stöber–Fink–Bohn method and a rapidly seeded growth. The hydroxyl-functionalized ligands on QDs ensured the effective trapping of the QDs in the silica matrix instead of adsorbing it on the surface of the silica sphere.

dx.doi.org/10.1021/am500429c | ACS Appl. Mater. Interfaces 2014, 6, 5744–5748

In addition, the rapid seeding technique, quite interestingly, trapped a number of QD particles of about 3 nm in size in spherical silica of about 230 nm in diameter, as shown in Figure 1c. To validate the possibility of chemical reactions between $CuInS_2$/ZnS QDs and silica, the chemical compositions of QDES were measured by energy-dispersive X-ray spectroscopy, and the results are shown in Figure 1d. Energy-dispersive spectra (EDS) show all of the elements, including sulfur, in expected ratios, and no chemical reaction between $CuInS_2$/ZnS QDs and silica could be inferred.

Figure 2 shows the thermal stability of QDES in comparison to that of QDs. As the temperature is increased from room

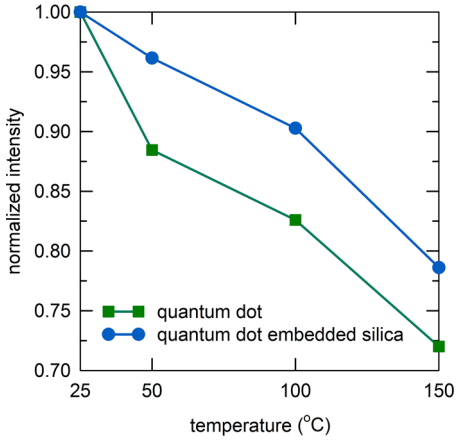

Figure 2. Thermal quenching characteristics of QDES in comparison to QDs.

temperature to 150 °C, the emission intensities of QDES were reduced more smoothly than those of QDs. Generally, QDs have low thermal stability. When the temperature is increased, oxides formed are diffused to QD's core and cause photo-oxidation. In comparison to QDs, QDES has a silica matrix as a buffer, which absorb damages from thermal shock. Although the stability of QDES was improved, further enhancement is required to reduce the thermal damages of QDs from LED chips.

Generally, LED chips are prepared by silicon resin, dispersed in phosphor as an encapsulant. In this case, phosphor in silicone resin undergoes thermal stress directly and reduces LED efficiency. Therefore, we propose a new concept of the WLED package by stacked QDES film on a robust phosphor plate. To improve the stability, QDESs were packaged as a film by dispersing QDES in ETPTA resin at a ratio of 8:2 by weight. About 0.4 mm thick films were achieved. The film was of uniform thickness and shows optical transparency in the visible region of the spectrum, indicating that QDES powders were well-dispersed in ETPTA films. To make WLED, the above Q-ETPTA films, which emit orange light, and the YAG:Ce^{3+} phosphor plate prepared by dispersing YAG:Ce^{3+} phosphor in a glass frit were used in remote phosphor configuration. For a comparative analysis, we also synthesized YAG:Ce^{3+} film by dispersing the phosphor in ETPTA (Y-ETPTA). Remote phosphor configuration, which maintains appreciable distance between blue/UV emitting chip and color converters, does the least damage to them, in addition to providing smooth chromaticity variation and enough diffusing effect by concealing the point source.

To start with, in terms of luminescence, the least favorable configuration of stacking the Q-ETPTA film, the above Y-ETPTA, was used, because the operating temperature of LEDs could damage the QDES in the long run as a result of direct heat from the LED chip, if a reverse order is used. However, it was observed that luminous efficacy of the WLED system prepared from the mixture was less compared to that of separate films stacked one over the other. Even though the Q-ETPTA floating film stacked over Y-ETPTA on the LED chip was delivering higher CRI and efficacy, the arrangement could not immaculately prevent thermal shock imparted on QDES by the LED chip. To overcome the thermal effect, we applied a new type of packaging in remote phosphor configuration using PiG. Instead of the ETPTA resin matrix, a PiG with YAG:Ce^{3+} phosphor having a higher thermal resistivity was used. Prototype WLEDs were fabricated using a surface-mounted-type InGaN-based blue-emitting (450 nm) LED employing remote phosphor configuration. PiG plates were prepared from YAG:Ce^{3+} and glass frit and polished to an appropriate thickness before stacking with Q-ETPTA, and the arrangement was fixed on top of a LED chip, as shown in Figure 3c. In this

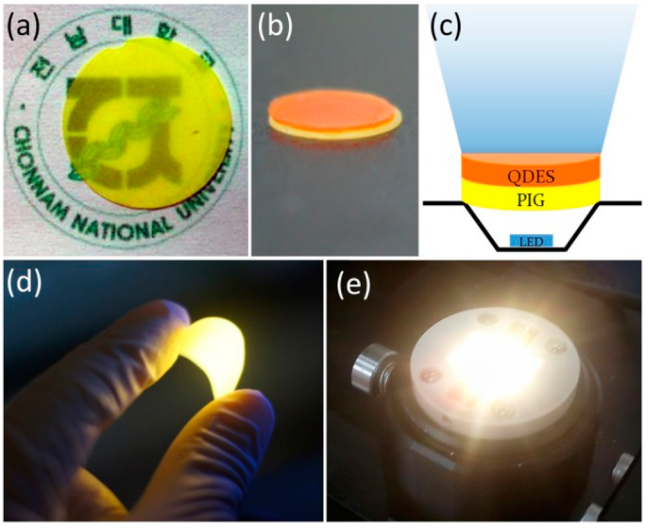

Figure 3. (a) Photograph of PiG. (b) Q-ETPTA film stacked on PiG. (c) Schematic diagram of the WLED. (d) Photograph of Q-ETPTA film under UV illumination. (e) WLED under operation.

configuration, the PiG plate, which itself maintains an appreciable distance from the chip, was placed between the LED chip and QDES films. Because the PiG plate is placed far from the LED chip, heating of the phosphor is considerably reduced and, in addition, the PiG plate, which has a lower thermal conductivity, maintains a higher temperature gradient across it and blocks the thermal stress on the QDES from the LED chip.[20] Moreover, PiG withstands and protects ETPTA from the usual photo-induced damages on the packaging materials caused by unconverted high-energy radiations traversing through it. All of these together ensure supreme spectral and mechanical stability of the WLED system over time. Figure 4 shows the EL of WLEDs fabricated using stacked Q-ETPTA over PiG under various forward bias current values. The image in the inset of Figure 4 shows the CIE color coordinates of the four different WLEDs fabricated, viz., PiG + Q-ETPTA, Y-ETPTA + Q-ETPTA, QDES-YAG, and QD-YAG systems. The proposed WLED configuration using PiG and Q-

dx.doi.org/10.1021/am500429c | ACS Appl. Mater. Interfaces 2014, 6, 5744−5748

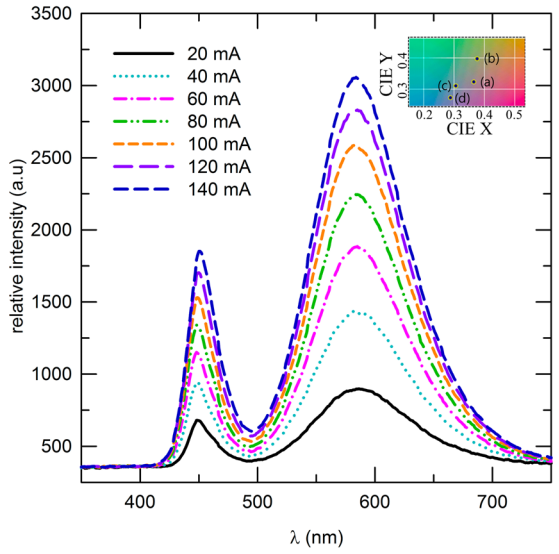

Figure 4. EL spectra of PiG−Q-ETPTA converted WLED. The inset shows CIE color coordinates corresponding to (a) stacking of Q-ETPTA over PiG, (b) stacking of Q-ETPTA over Y-ETPTA, (c) YAG + QDES conformal LED, and (d) YAG + QD conformal LED system.

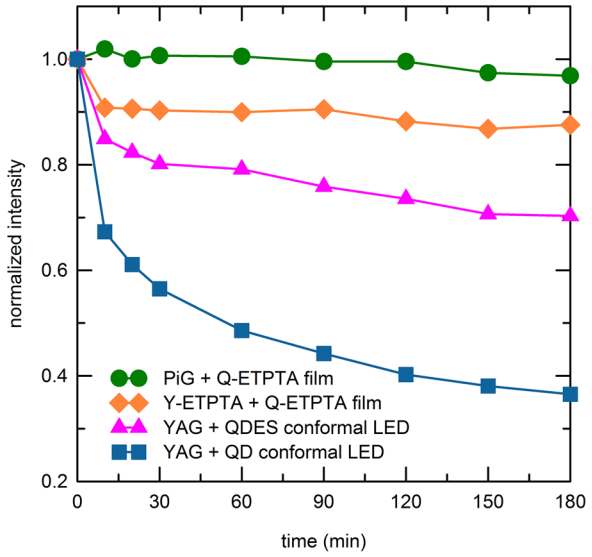

Figure 5. Peak emission intensity plot of the proposed PiG + Q-ETPTA system in comparison to Y-ETPTA + Q-ETPTA, YAG + QDES conformal LED, and YAG + QD conformal LED.

ETPTA shows white-light emission with CIE color coordinates of (0.363, 0.324) and CRI of 91 under a bias current of 20 mA. Spectral details of other configurations along with representative configuration are tabulated in Table 1.

Table 1. EL Properties of WLEDs Fabricated

sample configuration	CIE *x*	CIE *y*	R_a	luminous efficiency (lm/W)
PiG + Q-ETPTA	0.363	0.324	91	3.72
Y-ETPTA + Q-ETPTA	0.374	0.397	83	2.91
YAG + QDES conformal LED	0.304	0.311	83	6.38
YAG + QD conformal LED	0.285	0.273	79	4.03

Instead of stacking Q-ETPTA over PiG, a much more desirable configuration of PiG−Q-ETPTA units could be prepared by applying ETPTA along with the photoinitiator on the polished PiG surface, compressing the Q-ETPTA on it with a suitable load, and subsequently, exposing the arrangement in UV radiation. The later arrangement could avoid the air interface between PiG and Q-ETPTA, and the refractive dispersion losses arising from it could be further eliminated. However, in this study, the Q-ETPTA was simply stacked on PiG and EL stability of the floating film arrangement was analyzed. Figure 5 shows time-dependent EL peak intensity against time for different configurations of WLED. The conformal LEDs using YAG:Ce^{3+} and QDs exhibited 36% of initial intensity, while the combination of YAG:Ce^{3+} and QDES exhibited 70% of initial intensity. In the case of the Y-ETPTA and Q-ETPTA combination, as the operating time increases, thermal stress arises and degrades the luminescence as much as 30% of the initial emission intensity. However, usage of PiG results is outstanding and invariant, maintaining 97% of the initial intensity.

CONCLUSION

To conclude, we have successfully developed a new packaging technique for using QDs as color converters. The configuration provides excellent color rendering and protects the QDs from vulnerable operation conditions, such as thermal decomposition, oxidation, etc. In addition, the proposed configuration provides the highest luminous efficiency among the studied configurations.

AUTHOR INFORMATION

Corresponding Author

*Telephone: +82-62-530-1715. Fax: +82-62-530-1699. E-mail: imwonbin@jnu.ac.kr.

Author Contributions

§Both authors contributed equally to this work.

Notes

The authors declare no competing financial interest.

ACKNOWLEDGMENTS

This research is supported by the Ministry of Education, Science, and Technology (MEST) and the National Research Foundation of Korea (NRF) through the Human Resource Training Project for Regional Innovation. This work was also supported by the Strategic Key-Material Development and the Materials and Components Research and Development bodies, funded by the Ministry of Knowledge Economy (MKE, Korea).

REFERENCES

(1) Suehiro, T.; Hirosaki, N.; Xie, R. J. Synthesis and photoluminescent properties of $(La,Ca)_3Si_6N_{11}:Ce^{3+}$ fine powder phosphors for solid-state lighting. *ACS Appl. Mater. Interfaces* **2011**, *3*, 811−816.

(2) Lorbeer, C.; Mudring, A. V. White-light-emitting single phosphors via triply doped LaF_3 nanoparticles. *J. Phys. Chem. C* **2013**, *117*, 12229−12238.

(3) Zhang, J. Z. Challenges and opportunities in light and electrical energy conversion. *J. Phys. Chem. Lett.* **2011**, *2*, 1351−1352.

(4) Uheda, K.; Hirosaki, N.; Yamamoto, H. Host lattice materials in the system Ca_3N_2−AlN−Si_3N_4 for white light emitting diode. *Phys. Status Solidi* **2006**, *203*, 2712−2717.

(5) Dhanaraj, J.; Jagannathan, R.; Trivedi, D. C. $Y_2O_2S:Eu^{3+}$ nanocrystals—Synthesis and luminescent properties. *J. Mater. Chem.* **2003**, *13*, 1778−1782.

(6) Mahamuni, S.; Lad, A. D.; Patole, S. Photoluminescence properties of manganese-doped zinc selenide quantum dots. *J. Phys. Chem. C* **2008**, *112*, 2271−2277.
(7) Shiohara, A.; Hanada, S.; Prabakar, S.; Fujioka, K.; Lim, T. H.; Yamamoto, K.; Northcote, P. T.; Tilley, R. D. Chemical reactions on surface molecules attached to silicon quantum dots. *J. Am. Chem. Soc.* **2009**, *132*, 248−253.
(8) Hao, W.; Kyu Seung, L.; Jae Hyoung, R.; Chang Hee, H.; Yong Hoon, C. White light emitting diodes realized by using an active packaging method with CdSe/ZnS quantum dots dispersed in photosensitive epoxy resins. *Nanotechnology* **2008**, *19*, 145202.
(9) Yue, F.; Tomm, J. W.; Kruschke, D.; Glas, P. Stimulated emission from PbS-quantum dots in glass matrix. *Laser Photonics Rev.* **2013**, *7*, L1−L5.
(10) Sonawane, R. S.; Naik, S. D.; Apte, S. K.; Kulkarni, M. V.; Kale, B. B. CdS/CdSSe quantum dots in glass matrix. *Bull. Mater. Sci.* **2008**, *31*, 495−499.
(11) Liu, C.; Heo, J.; Zhang, X.; Adam, J.-L. Photoluminescence of PbS quantum dots embedded in glasses. *J. Non-Cryst. Solids* **2008**, *354*, 618−623.
(12) Subila, K. B.; Kishore Kumar, G.; Shivaprasad, S. M.; George Thomas, K. Luminescence properties of CdSe quantum dots: Role of crystal structure and surface composition. *J. Phys. Chem. Lett.* **2013**, *4*, 2774−2779.
(13) Kwak, S. K.; Yoo, T. W.; Kim, B. S.; Lee, S. M.; Lee, Y. S.; Park, L. S. White LED packaging with layered encapsulation of quantum dots and optical properties. *Mol. Cryst. Liq. Cryst.* **2012**, *564*, 33−41.
(14) Bozyigit, D.; Yarema, O.; Wood, V. Origins of low quantum efficiencies in quantum dot LEDs. *Adv. Funct. Mater.* **2013**, *23*, 3024−3029.
(15) Lin, C. C.; Liu, R.-S. Advances in phosphors for light-emitting diodes. *J. Phys. Chem. Lett.* **2011**, *2*, 1268−1277.
(16) Huang, C. H.; Chan, T. S.; Liu, W. R.; Wang, D. Y.; Chiu, Y. C.; Yeh, Y. T.; Chen, T. M. Crystal structure of blue−white−yellow color-tunable $Ca_4Si_2O_7F_2$:Eu^{2+},Mn^{2+} phosphor and investigation of color tunability through energy transfer for single-phase white-light near-ultraviolet LEDs. *J. Mater. Chem.* **2012**, *22*, 20210−20216.
(17) Kim, H.; Jang, H. S.; Kwon, B. H.; Suh, M.; Youngsun, K.; Cheong, S. H.; Jeon, D. Y. In situ synthesis of thiol-capped $CuInS_2$-ZnS quantum dots embedded in silica powder by sequential ligand-exchange and silanization. *Electrochem. Solid-State Lett.* **2011**, *15*, K16−K18.
(18) Song, W. S.; Yang, H. Efficient white-light-emitting diodes fabricated from highly fluorescent copper indium sulfide core/shell quantum dots. *Chem. Mater.* **2012**, *24*, 1961−1967.
(19) Kim, H.; Suh, M.; Kwon, B. H.; Jang, D. S.; Kim, S. W.; Jeon, D. Y. In situ ligand exchange of thiol-capped $CuInS_2$/ZnS quantum dots at growth stage without affecting luminescent characteristics. *J. Colloid Interface Sci.* **2011**, *363*, 703−706.
(20) Lee, J. S.; Unithrattil, S.; Kim, S.; Lee, I. J.; Lee, H.; Im, W. B. Robust moisture and thermally stable phosphor glass plate for highly unstable sulfide phosphors in high-power white light-emitting diodes. *Opt. Lett.* **2013**, *38*, 3298−3300.
(21) Lee, Y. K.; Lee, J. S.; Heo, J.; Im, W. B.; Chung, W. J. Phosphor in glasses with Pb-free silicate glass powders as robust color-converting materials for white LED applications. *Opt. Lett.* **2012**, *37*, 3276−3278.